Universiteit Utrecht

Universiteit Utrecht
Erasmus University Medical Center

DEVELOPMENT OF HER2-TARGETED THERANOSTICS FOR DIAGNOSIS AND TREATMENT OF BREAST CANCER

Minor Internship Final Report

Yijun Hu

Supervisors:	Yann Seimbille (Ph.D)
	Priciana Paraiso (Pharm.D)
Second reviewer:	Bertrand Kleizen (Ph.D)

October 2022
Department of Radiology & Nuclear Medicine, Erasmus University Medical Centre
Dr. Molewaterplein 40, 3015 GD Rotterdam

ABSTRACT

A library of peptides targeting HER2 was established from *in silico* docking analysis of a pool of over 8000 preliminary sequences based on a recently developed anti-HER2 peptide KSPNPRF. The library has been synthesized by solid-phase Fmoc protocol and evaluated for their binding affinities. The peptides have a common core sequence, PNP, flanked by various amino acids and conjugated to a Cy5.5 fluorescent dye via a PEG_4-K linker. Six peptides of this library have been evaluated by a magnetic beads-based fluorescence binding assay and compared to the reference KSPNPRF and a scrambled control peptide developed by the same group. With this assay, we found a K_D of 49 nM for the reference, while the affinities of the six peptides of the library ranged from ~40 nM to ~2 μM. However due to the ambiguity of the data analysis, these values need to be further validated. We also report the development of a surface plasmon resonance protocol to evaluate the peptide library. For this, we have immobilised biotinylated HER2 on a streptavidin-coated chip and assessed the effect of the protein type, sensor chip, and regeneration conditions on the quality of the measurements of the KSP*, scrambled control peptide and Herceptin. While the SPR signal is sufficient, further investigations are needed to reduce non-specific binding and improve the signal quality.

LAYMAN'S SUMMARY

To date, breast cancer is still the most diagnosed type of cancer in women worldwide. In some patients with aggressive types of breast cancer, scientists have found that the human epidermal growth factor receptor 2 (HER2) is quantitatively increased. HER2 has therefore become a useful target for diagnosis and treatment of breast cancer. In this report, we have synthesized 9 peptides based on a recently developed peptide that targets HER2. We synthesized these peptides and labelled them with a fluorescent dye called Cy5.5. Because of the fluorescence, we could quantitatively measure the amount of binding to HER2 and determine the affinity to HER2 in a binding assay where HER2 was immobilised on magnetic beads. We have tested six compounds of the library and found binding affinities ranging from ~40 nM to ~2 μM. Due to inaccuracies found in the analysis, further experiments are needed to confirm the results. We also explored another method to determine the binding affinity of the peptides to HER2, using surface plasmon resonance (SPR) technology. In this method, HER2 was bound onto a special sensor chip which was placed inside the SPR instrument. After injection of the peptides, the binding to HER2 is measured by recording the increase of mass at the chip surface. We have tested various conditions and analysed its effects on the measurements. However, optimisation is needed to correct the data for non-specific binding and signal quality.

TABLE OF CONTENTS

INTRODUCTION AND BACKGROUND

Breast cancer is the most common diagnosed cancer and also the leading cause of cancer-related deaths in women[1]. Breast cancer is a very heterogeneous type of tumour and can be classified into several categories based on receptor expression or the absence thereof. Breast cancer subtypes include those that express estrogen receptor (ER); and/or progesterone receptor (PR); human epidermal growth factor 2 receptor (HER2), and those that do not express any of these receptors[2]. Each cancer subtype has its own set of diagnostic and therapeutic challenges. However, like all malignancies, breast cancer benefits considerably from early identification before it spreads to other parts of the body.

HER2 is a unique marker for breast cancer

HER2 is a 185 kDa glycoprotein, part of the tyrosine kinase receptor family (ErbB) that also include HER1, HER3 and HER4[3]. The dysregulation of this receptor family has been seen in various types of cancers. Among the family members, HER2 is a unique receptor molecule with no natural ligand and functions as a co-receptor to form homo and hetero-dimers with other HER family members[3,4]. The dimerization results in the autophosphorylation of tyrosine residues in the cytoplasmic domain of the receptor. This in turn, initiates a variety of signalling cascades including MAPK and PI3K/AKT pathways that are responsible for cell proliferation, differentiation, migration and apoptosis[3].

The overexpression of HER2 is found in 15% to 25% of all breast tumours and is linked to aggressive tumour growth, increased metastasis potential, and poor prognosis[5]. Since the receptor can be overexpressed up to 2 million times greater than the normal basal level, the receptor can serve both as a diagnostic marker and a promising therapeutic target[6]. Accurate assessment of HER2 receptor status is crucial for identification of patients that would benefit most from HER2-targeted therapies.

At present, the two main diagnostic techniques to assess HER2 status are immunohistochemistry and fluorescence in situ hybridization, both requiring biopsies of suspected tissues[7]. While these techniques have been proven to be clinically useful, it is difficult to determine the heterogeneous nature of breast tumour tissues. There has also been increasing evidence that the status of primary tumours can be different from metastatic tissues, leading to inappropriate choice of treatment[8,9]. Moreover, both techniques are very invasive and not all tissues are accessible for biopsy. As a non-invasive diagnostic alternative, positron emission tomography (PET) imaging of HER2 can provide a full-body diagnosis and detection of HER2 expression.

Peptide based theranostics for HER2 positive breast cancers

In recent years, nuclear medicine has made great advancements in the development of imaging agents for visualisation and localisation of tumours and monitoring treatment response. The novel concept ‘theranostics’ involves ligands radiolabelled with gamma- or positron-emitting radionuclides for diagnostic purposes and makes use of the same ligand labelled with therapeutic alpha- or beta-emitting radionuclides to treat patients based on the preliminary diagnosis[10].

Currently many clinical trials for PET imaging of HER2 involve the use of monoclonal antibodies (mAb), i.e. trastuzumab and pertuzumab, to detect HER2 expression[11–13]. However, antibody-based targeting moieties have many drawbacks. With a molecular weight around 150 kDa, the large size of mAbs can hinder diffusion into tumour[14,15]. The slow pharmacokinetics associated with mAbs means that it takes days for significant levels to accumulate in tumours. For example, the ^{89}Zr labelled HER2-targeted mAb, currently in phase II clinical trials, can only be imaged 4-7 days after injection[16]. This also means that longer-lived isotopes must be used, increasing the exposure of patients and personnel to radiation.

Peptides, on the other hand, are significantly lower in molecular weight, have a faster circulation time in blood and decreased immunogenicity. Additional benefits of peptides as targeting vectors, include higher tumour penetration, higher stability, high tunability, ease of synthesis and lower

manufacturing costs [17]. HER2 positive cancers could therefore benefit from peptide-based agents which could decrease imaging times, resulting in faster and more accurate treatments as well as decreasing the of healthy tissues to cytotoxic radiation.

There have been a number of promising peptides against HER2 discovered[18]. The most recent study by Joshi *et al.* identified a peptide with the sequence KSPNPRF (KSP*), which was conjugated with a near-infrared fluorescent probe (FITC or Cy5.5) via a GGSK linker[19]. The peptide was evaluated for its specificity and affinity for the extracellular domain of HER2. It was found in *in vitro* experiments that KSP* binds to HER2 with a K_D of 21 nM and an association time constant of 0.14 min^{-1} [19]. The peptide has also been validated for real-time *in vivo* imaging in preclinical model of colorectal cancer.

Development of new peptides against HER2

When developing new peptides, the binding affinity of a ligand for a target is one of the most important properties. To determine the ligand binding affinity, some approaches require labelling prior to measurements in-solution, while others require capture of the ligand or target as is the case in sensor-based approaches[20]. One also decides whether the measurements are directly performed on cells, cell fragments or if the target needs to be extracted before measuring the ligand affinity. The former is more commonly employed due to its simplicity and the fact that the native environment of the target protein is maintained. While the second approach removes the protein from the native environment, it enables the researcher to have more control and ensures that only the protein of interest is to be investigated.

Specifically for this report, we discuss two approaches: magnetic beads-based fluorescence assay and surface plasmon resonance (SPR).

Magnetic beads-based fluorescence assay

While the pioneering radiolabelled ligand assays are extremely sensitive, allowing the determination of affinities in the picomolar range, they present many drawbacks. These include: the requirement of specific equipment, specialised and isolated laboratory space as well trained and certified personnel exposed to radioactive risks. For safety and practicality purposes during large-scale screening, there have been a rise in protocols involving fluorescence, including those based on the rotational speed of the fluorescent ligand (fluorescence polarization) and fluorescence resonance energy transfer (FRET) [21].

Most recently, Hattori et al. (2020) has reported a high-throughput fluorescence-based assay using magnetic beads. This assay measures the amount of fluorescently-labelled ligand bound to the target on the magnetic beads. The assay is an equilibrium binding assay based on the principles of Law of Mass Action: one of the reactants (target or ligand) is fixed at a low concentration and the other reactant is varied over a range of concentrations and allowed to come to equilibrium[22]. According to the Law of Mass Action, the ratio of the reactants are constant at equilibrium. From this, the dissociation equilibrium constant (K_D) can be defined as the ratio of free reactants over the formed complex. Therefore, by measuring the concentration of the formed complex, the K_D can be determined as the concentration reactant B (the one that is varied) required to convert half of the other reactant A into complex AB, according to the equation derived from the Law of Mass action.

$$\text{Fraction bound} = \frac{[\text{L}]}{[\text{L}] + K_\text{D}}$$

The fraction bound is the ratio of receptors bound to ligand and [L] is the ligand concentration at equilibrium. Plotting this equation against the various ligand concentrations, forms a rectangular hyperbola or binding isotherm, from which the K_D can be determined (**Fig. 1**, bottom left).

Surface plasmon resonance

Among the sensor-based approaches, surface plasmon resonance (SPR) has resurfaced as a robust and precise method for determining binding affinities. The technique measures real-time kinetics with high sensitivity without the need for labels[23,24]. The method of SPR involves immobilisation of the target protein on the surface of a sensor chip which has a single layer of dextran covalently coupled to a gold surface. The ligands of interest is then allowed to flow over the prepared surface. The SPR signal arises from changes in the refractive index at the surface of the gold sensor chip. Every binding event causes an increase in the mass at the surface, which in turn causes a proportional increase in the refractive index and therefore the change in response. These changes are measured as changes in the resonance angle ($\delta\theta$) of refracted light and quantified as resonance units (RU), where 1 RU is equal to critical angle shift of 10^{-4} degrees. Most importantly, the signal is linearly correlated to the total mass bound. The SPR experiment produces a sensorgram where RU is plotted over time. From this, one can observe the increase in signal due to formation of ligand-receptor complexes (association phase). After a certain time, a steady-state is reached, where the dissociation and association are in equilibrium. In the next step, the injection of (regeneration) buffer causes a decrease in signal until it is returned to baseline (dissociation phase), see **Figure 1**, right bottom panel. The sensorgram data is fitted into kinetic models from which the k_{on}, k_{off} and K_D can be determined.

Aim and design of this study

The anti-HER2 peptide discovered by Joshi *et al*. could be a promising radio-theranostic vector for imaging and treatment of HER2 positive breast cancers. However, *in vivo* imaging of the peptide injected in a mouse showed large non-specific uptake and signs of molecular instability (unpublished data). The peptide has to be improved before it could potentially be used as a theranostic vector against HER2 positive breast cancer. Therefore, the aim of the study is to synthesize and evaluate the binding of a library of new promising peptides, and to compare them with the reference KSP* peptide.

In this report, we show the synthesis and purification of a library of promising peptides designed to target HER2. The peptides were labelled with Cy5.5 and assessed for their binding affinities by a magnetic beads-based fluorescence assay and development of a SPR method. This study will facilitate the development of novel radio-theranostics against HER2-amplified cancers that could aid in early and late-stage diagnosis, treatment and monitor of therapy efficacy.

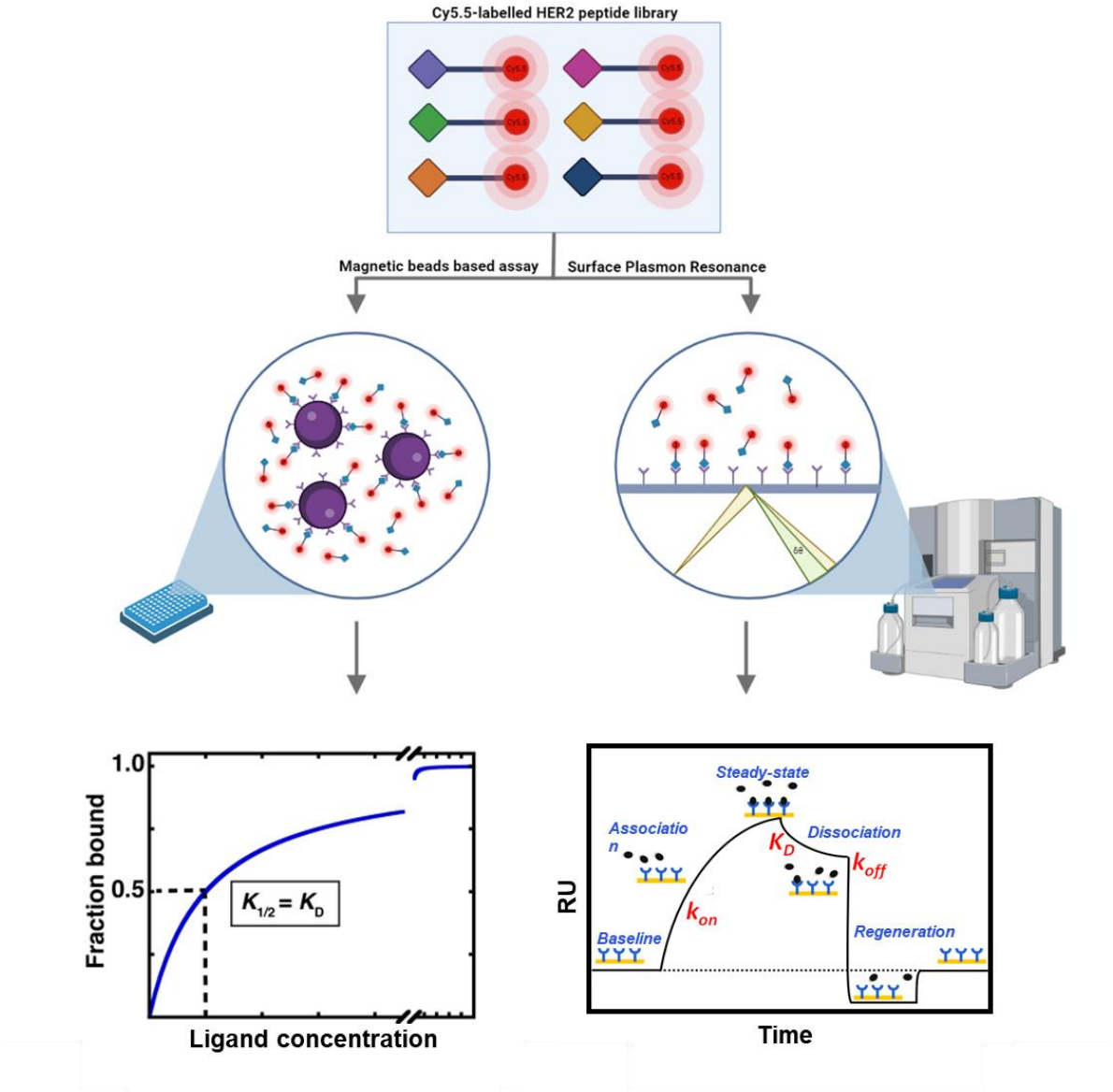

Figure 1 Overview of this study. The binding of the Cy5.5-labelled peptides against HER2 selected by molecular docking experiments will be evaluated by a magnetic bead-based assay (left) and surface plasmon resonance experiments (right).

EXPERIMENTALS

Materials - Peptide synthesis reagents were purchased from Aaptec, Bachem or Sigma-Aldrich. Phosphate-buffered saline (PBS) was diluted from a 10x commercial stock (Sigma Aldrich). All other chemicals and materials were obtained from Sigma-Aldrich unless stated otherwise.

Peptide library construction - The library of peptides was established from molecular docking experiments performed by my supervisors (Priciana and Yann). Briefly, a total of 8000 candidate peptides were generated and docked against HER2 ectodomain in HPEPDock. From this, the 9 peptides with highest docking scores were selected to be synthesized and further evaluated.

Peptide synthesis - All peptides were synthesized according to standard Fmoc-based solid-phase synthesis protocols. Fmoc-, Boc- protected L-amino acids or Fmoc-NH-PEG_4-COOH (4 equivalents relative to the loading of the resin) were used for the elongation of the peptide on the resin and each coupling was monitored with ninhydrin test. All coupling reactions were carried out in dimethylformamide (DMF) while gently shaking at room temperature. The peptides are all conjugated on either the N-terminus or the C-terminus with Cy5.5 via a 4-unit polyethylene glycol linker (PEG_4). The general synthesis scheme is shown in **Figure S1**.

For the peptides labelled on the C-terminal lysine, pre-swelled rink amide MBHA resin (Novabiochem, 0.13 g dry weight) was deprotected with 20% piperidine solution in DMF (2 x 15 min) and Fmoc-Lys(ivDde)-OH was loaded onto the resin with HBTU (3.9 eq.), OxymaPure (4 eq.) and DIPEA (8 eq.) overnight. The peptides were elongated in cycles of deprotection (20% piperidine, 2 x 15 min) and coupling (3.9 eq. HBTU 4 eq. OxymaPure, 8 eq. DIPEA, 2 h). The final N-terminal amino acid was Boc-protected to prevent undesired Fmoc removal during the deprotection of ivDde prior to labelling. Finally, the ivDde protecting group was removed with 5% hydrazine (4 x 1 h).

For the peptides labelled on the N-terminal lysine, pre-swelled rink amide resin (Novabiochem, 0.13 g dry weight) was deprotected with 20% piperidine (2 x 15 min) and the first amino acid was loaded onto the resin overnight with HATU (4 eq.) and DIPEA (8 eq.). The peptides were elongated in cycles of deprotection (20% piperidine, 2 x 15 min) and coupling (4 eq. HATU, 8 eq. DIPEA, 2 h). The final N-terminal lysine was incorporated as Boc-Lys(Fmoc)-OH and the Fmoc-protecting group was removed using 20% piperidine (2 x 15 min).

After the deprotection of the lysine residue, the resin was washed 5 times with DMF and labelled with 1 eq. Cy5.5 NHS ester (Lumiprobe) in the presence of DIPEA (8 eq.) overnight. The peptides were cleaved from the resin using a TFA/H_2O/TIPS cocktail (95:2.5:2.5) for 3 h while shaking at room temperature. The peptides were precipitated in cold diethylether and centrifuged at 7000 rpm for 15 min. After removing the diethylether, the dried crude peptides were dissolved in acetonitrile:water (v/v, 35/65) and purified using HPLC (Agilent Technologies) with a gradient of water + 0.1% formic acid (FA) and acetonitrile + 0.1% FA. The purity of the peptides was determined by LC-MS (Agilent Technologies) in positive ion mode.

Magnetic beads binding assay - Human HER2-coupled magnetic beads (MBS-K006, Acrobiosystems) were reconstituted according to manufacturer's instructions. The beads were washed once using a magnetic stand and diluted in phosphate-buffered saline (pH 7.4) supplemented with 0.1% bovine serum albumin (PBS-B) to a bead concentration of 0.1 mg/mL. For the non-specific binding control, Dynabeads MyOne™ streptavidin T1 magnetic beads (ThermoFisher) were washed and diluted to 0.1 mg/mL in the same way.

Peptides were diluted in PBS-B to concentrations ranging from 10^{-10} M to 10^{-5} M from a 10^{-3} M stock in DMSO. The screening for each peptide was performed in triplicate. Peptides (100 µL) at various concentrations were mixed with HER2 beads or streptavidin beads suspension (5 µL) in a 96-well PCR plates (ThermoFisher, AB0700). As a blank control, PBS-B was mixed with beads. The plates were allowed to incubate for 1.5 h at 25 °C while agitating on an Eppendorf Thermomixer C (1300 rpm). The

magnetic beads were pulled to the bottom of the wells on a 96-well magnetic stand before the supernatant is carefully removed. To wash the beads, PBS supplemented with 0.05% Tween-20 (100 µL; PBS-T) was added to each well, agitated for 5 minutes and put back on the magnetic stand before removal of the supernatant. This step was repeated four times. After the final wash, the beads were resuspended in PBS-B (100 µL), placed on a PCR plate holder and analysed by the Hidex Sense platereader. The samples were excited with the 655 nm filter and detected via the 710 nm emission filter using 100 flashes at high power. The entire protocol was performed in the dark to avoid degradation of the probe.

The data was exported and the binding curve was fitted in Graphpad Prism via non-linear regression of 1:1 binding model. This regression analysis fits a Agonist versus response sigmoidal curve to determine 4 parameters: Top plateau value (saturation), Bottom plateau value, Hill slope and EC50 (effective concentration at half maximum). The results were corrected according to a standard calibration curve of Cy5.5 and normalised to lowest mean values. The screening of each peptide was performed twice.

Surface plasmon resonance experiments - Biacore CM5 sensor chips (GE Healthcare Life Sciences) and Series S sensor chip SA (Cytiva Life Sciences) were used for surface plasmon resonance (SPR) studies. Streptavidin was immobilised on CM5 sensor chip with an immobilisation level of 2500, controlled with the Biacore T100 software. Human biotinylated HER2 with long spacer (HE2-H822R, Acrobiosystems) or human biotinylated Avi-tag (HE2-H82E2, Acrobiosystems) was diluted in filtered running buffer (PBS-T), to a final concentration of 2 µg/mL. The proteins were immobilised onto the streptavidin-coated chips at a flow rate of 50 µL/minute.

Test compounds were diluted in running buffer and injected over the sensor surface at a flow rate of 50 µl/minute. In the first experiment, the surface was regenerated with 10 mM glycine (pH 1.5) in initial experiments. In later experiments, the surface was regenerated with running buffer. SPR binding analyses for binary complexes were performed in multi-cycle kinetics mode at 25°C.

For each test compound, SPR raw data in the form of resonance units (RU) were plotted as sensorgrams using the Biacore T100 control software. The signal from the blank sensorgram (reference flow cell) was subtracted from that of the test compound sensorgram.

RESULTS

Peptide library

From preliminary docking analyses conducted by my supervisors, it was found that the binding moiety PQP had a higher docking score than the original PNP sequence of KSP*. From this, a selection of PQP peptides with different amino acid sequences and conjugation of a probe at either C or N terminus has been made **(Table S1)**. The 9 selected peptides have better docking scores than the reference peptide KSP* and therefore promising candidates to evaluate experimentally.

Each peptide in the library was synthesized and conjugated with Cy5.5 to the side chain of a lysine residue on a PEG_4 linker (PEG_4-K). The choice to incorporate this linker rather than the GGGSK linker used originally for the KSP* is due to cost and time effective reasons. The added flexibility of the PEG_4 linker could also hypothetically improve the interaction of the binding moiety with HER2. Most of the peptides have been obtained at minimum 95% chemical purity, except for peptides 1 and 7 (**Fig 2, Fig. S2**). To evaluate the influence of the linker on the binding affinity, the GGGSK linker of the KSP* peptide was modified to PEG_4-K. This variant (reference 2), as well as the original reference peptide KSP* and the scrambled control peptide PPS*, were all successfully obtained at required purities of greater than 95% (**Fig. 2A**).

A

ID	Compound	MW (g/mol)	Yield (%)	Purity
ref-1*	KS**PNP**RF-GGGS-K(Cy5.5)-NH2	1796,1775	21,2	≥95%
ref-2	KS**PNP**RF-PEG4-K(Cy5.5)-NH2	1785,2345	23,9	≥95%
n.c.*	PPSNFKR-GGGS-K(Cy5.5)-NH2	1796,1775	22,9	≥95%
1	CFR**QPQP**QSFC-PEG4-K(Cy5.5)-NH2	2280,8035	15,3	<95%
2	**YQPQP**RF-PEG4-K(Cy5.5)-NH2	1875,3155	15,2	≥95%
3	FR**QPQPQSY**-PEG4-K(Cy5.5)-NH2	2090,5245	58,6	≥95%
4	**YSQPQPQ**RF-PEG4-K(Cy5.5)-NH2	2090,5245	18,0	≥95%
5	**FSQPQPQ**RFC-PEG4-K(Cy5.5)-NH2	2177,6645	27,7	≥95%
6	K(Cy5.5)-PEG4-**YQ**QPQPQRF-NH2	2131,5775	7,3	≥95%
7	K(Cy5.5)-PEG4-C**FSQPQPQ**RFC-**NH2**	2280,8035	16,6	<95%
8	K(Cy5.5)-PEG4-**FR**QPQPRF-NH2	2015,5055	27,8	≥95%
9	K(Cy5.5)-PEG4-**FRQPQPQ**RF-NH2	2144,6205	41,7	≥95%

* Joshi *et al.* (2016)

B

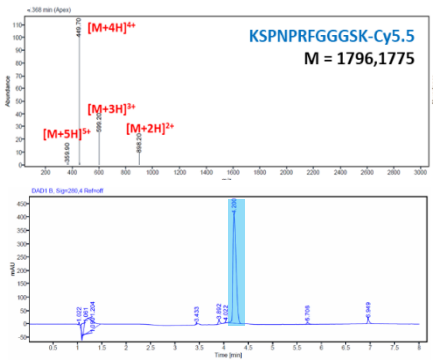

Figure 2 List of peptides synthesized by Fmoc-solid phase synthesis. (**A**) Including two reference peptides (ref-1 and ref-2), scrambled control peptide (negative control, n.c.) and the library of 9 new promising peptides against HER2. The purities were determined by LC-MS. The maximum obtained yields were calculated over all synthesis steps. (**B**) Exemplary LC-MS characterisation of ref-1 in positive ion mode.

Magnetic bead-based ligand screening of the peptide library

To evaluate the library, the binding affinity to HER2 was determined via fluorescence after incubating various dilutions of each peptide with HER2-coupled magnetic beads. The dilutions were also simultaneously incubated with streptavidin-coated beads to determine the amount of non-specific binding. While this binding assay is largely based on the binding assay described by Hattori *et al.* (2020), the original method has been optimised to fit the conditions required for the protein, the magnetic beads and fluorescence measurements. A standard curve with Cy5.5 NHS ester was produced to correct the concentrations of the dilutions (**Fig. S3**). Because the magnetic beads used for the non-specific binding control are not exactly identical to the beads coupled to HER2, all data shown are representative of the total binding rather than the specific binding. Moreover, other non-specific binding, such as to the wells, has not been corrected for. Therefore, the non-specific binding data serves to compare the binding levels of the ligand to the target HER2 versus non-HER2.

As shown in **Figure 3**, the binding assay determined an affinity of 41.2 nM for KSP*, while no binding could be determined for PPS*. For reference 2, we have determined a binding affinity of 49.7

nM, which is in the same range as KSP* (**Fig. 3A**). While these numbers are slightly higher than the reported values by Joshi et al, it is nonetheless within the nanomolar range and any deviation could be justified by the significant differences in the methods.

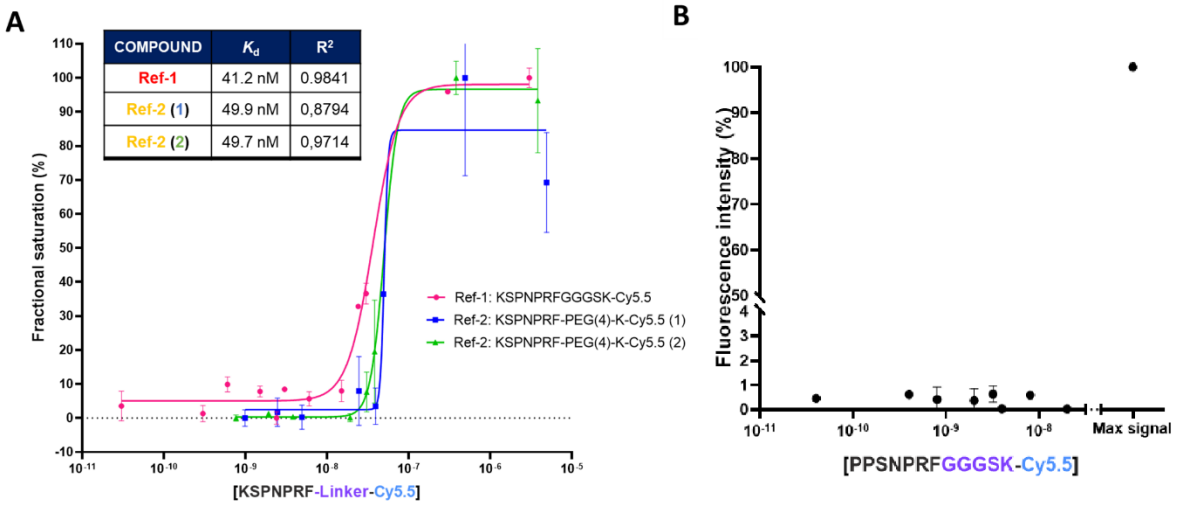

Figure 3 Magnetic bead-based ligand screening of KSP* and PPS* against HER2. The binding affinity of the reference peptides KSP* (Ref-1) and KSPNPRF-PEG$_4$-K-Cy5.5 (Ref-2, in duplicate) (**A**) and scrambled control peptide (**B**) to HER2 was detected via fluorescence and measured in triplicate. For (**A**), the curves were fitted via a linear regression of a 1:1 binding model with the errors showing s.d. The K_D-values and the R^2 are calculated from the fitted curves and summarised in corresponding table. For (**B**), the data has been normalised to the maximal saturation signal.

From the library, six peptides were screened for binding to HER2-coupled magnetic beads. Summarised in **Fig. 4**, we found that none of the six screened peptides have affinities close to or better than that of reference 2. Peptide FRQPQPQSY* appeared to have a similar affinity as the reference in the first attempt, however this could not be reproduced in the second screening. The K_D-values found for other peptides could also not be accurately reproduced. Moreover, some of non-linear regression analyses have been denoted as "ambiguous" by Graphpad (K_D values with tilde symbol, **Fig. S4**). The data points suffer from great standard deviations, especially at higher end of the concentration range. It is likely explaining that some of the fits have become too ambiguous to interpolate accurate K_D-values. It is also worth noting that FSQPQPRFC* and YSQPQPQRF* were found to have high non-specific binding (**Fig. S4**). The calculated affinities of these peptides likely deviate even more from the actual values.

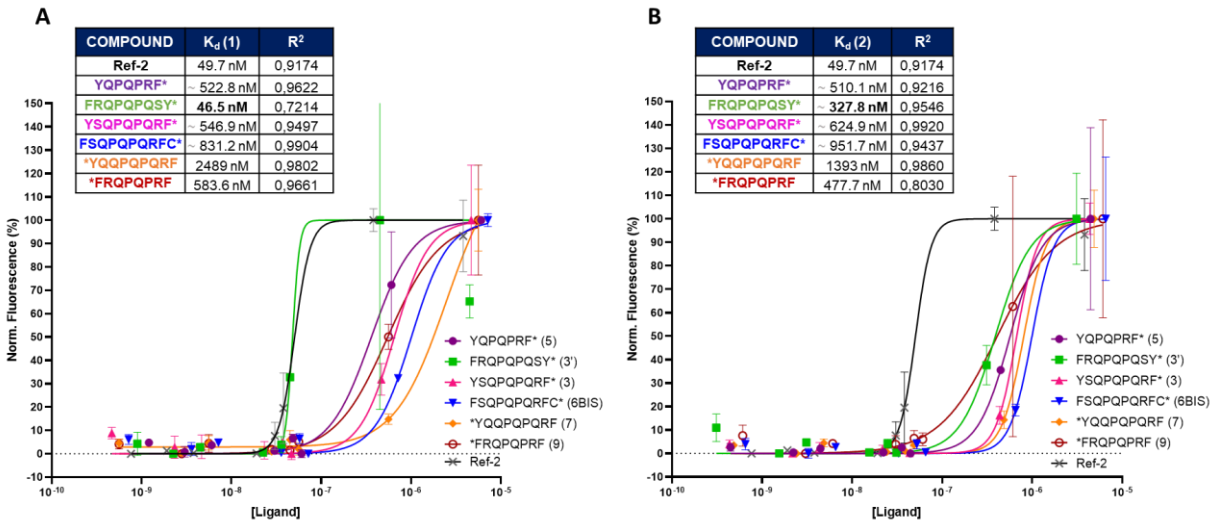

Figure 4 Magnetic bead-based ligand screening of peptide library against HER2. Total binding of the peptide library to HER2 was detected via fluorescence and measured in triplicate on two independent days, each shown separately in (**A**) and (**B**). Curves were fitted via a linear regression of a 1:1 binding model with the errors showing s.d. The K_D-values and the R^2 fit are calculated from the fitted curves and summarised in corresponding tables. The tilde (~) denotes "ambiguous" values.

Surface plasmon resonance binding experiments of KSP to HER2*

In parallel, we explored SPR on the Biacore T100 with the intention to compare the two approaches in determining the affinity of our ligands. By taking into account the kinetic parameters of both association and dissociation, SPR determines affinities more robustly and accurately than most common binding assays. However, due to the low molecular weight of peptides (~2 kDa), the change in refractive index of every binding event, and therefore the signal, is very minimal. Our attempts to optimise a method have therefore been mainly focused on gaining sufficient SPR signal.

In the first experiments, CM5 SPR sensor chips were coated with streptavidin via the wizard included with the instrument software. Biotinylated human HER2 (primary amine labelled) was immobilised until maximum saturation, reaching approximately 2000 RU. Then, cycles of association and dissociation of KSP* peptide dilutions were measured. While the manufacturer suggested regeneration of the surface with 10 mM glycine.HCl (pH 1.5), we found that milder conditions with running buffer (PBS-T) were enough to bring the signal back to baseline and slightly improved the signal (**Fig. S5**). As shown in **Figure 5A**, the resulting sensorgram contains bulk shift spikes at injections of buffer. Even more unusual is that the association phase does not reach a stable steady-state and starts to decrease halfway before the dissociation phase. It was therefore difficult to accurately model the kinetics and to calculate the K_D. Moreover, the maximal association phase signal is also well below the expected 15 RU. In fact, higher peptide concentrations resulted in saturation of a maximal association signal around 5 RU. We also noticed that the signal does not follow an association plateau, but starts decreasing slightly. This can be explained by the increase of non-specific binding observed in the reference flow cell, where the non-specific signal starts to exceed the specific signal at peptide concentrations higher than 625 nM (**Fig. S6**). Similar phenomena were also observed for PPS* (**Fig. 5B**). However, when comparing the concentrations below 625 nM, it becomes clear that PPS* interacts in a different manner with HER2 compared to KSP*; the signal increases during association, but it rapidly returns to baseline. Herceptin, on the other hand, show very strong association data, in concordance with literature reports (**Fig. 5C**).

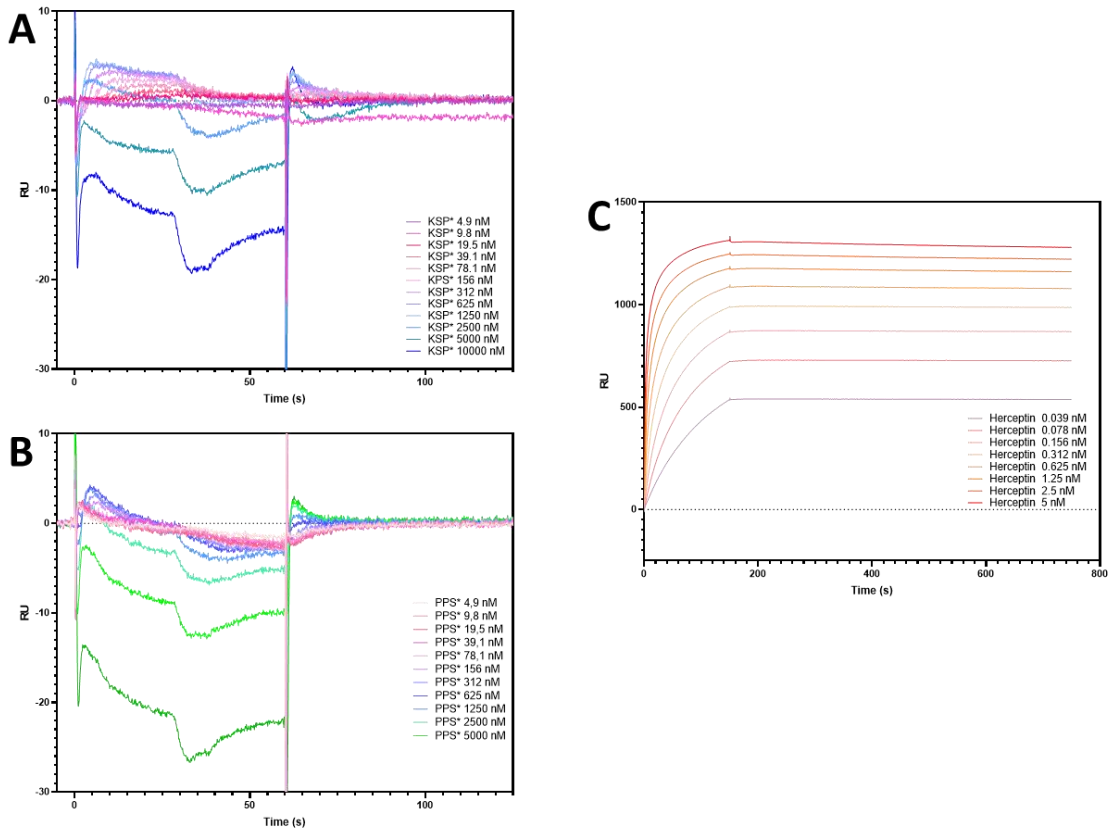

Figure 5 SPR analysis of immobilised HER2 on streptavidin-coated Cytiva CM5 Sensor Chip to serially diluted KSP* (A), PPS* (B) and Herceptin (C). Biotinylated HER2 with long spacer on primary amines was immobilised on the chip with levels of approximately 2100 RU. The chip surface was regenerated with running buffer (PBS-T) after 60 seconds of association time.

Figure 6A and B show sensorgrams obtained from experiments on Sensor Chip SA on which streptavidin has been pre-coupled for the immobilisation of biotinylated HER2. During the run of the highest concentration KSP*, the sensorgram falls to sub-zero values. This could likely be artefacts coming from oversaturation of the peptides on the chip. In the insets of **Figure 6A and B**, the highest concentrations have been omitted to show the differences between the binding of KSP* versus PPS* to HER2 more clearly.

From these results, we had hypothesized that the multi-biotinylated HER2 protein, biotin was attached to multiple primary amines on HER2, might mask potential binding sites. To test that theory, we purchased a mono-biotinylated Avitag HER2 protein (biotin connected at the C-terminus via an Avitag) and immobilised it onto the chip. Aside from reaching higher immobilisation level of the protein (nearly 3000 RU), the binding of the peptides to this variant showed no significant difference (**Fig. 6C and D**).

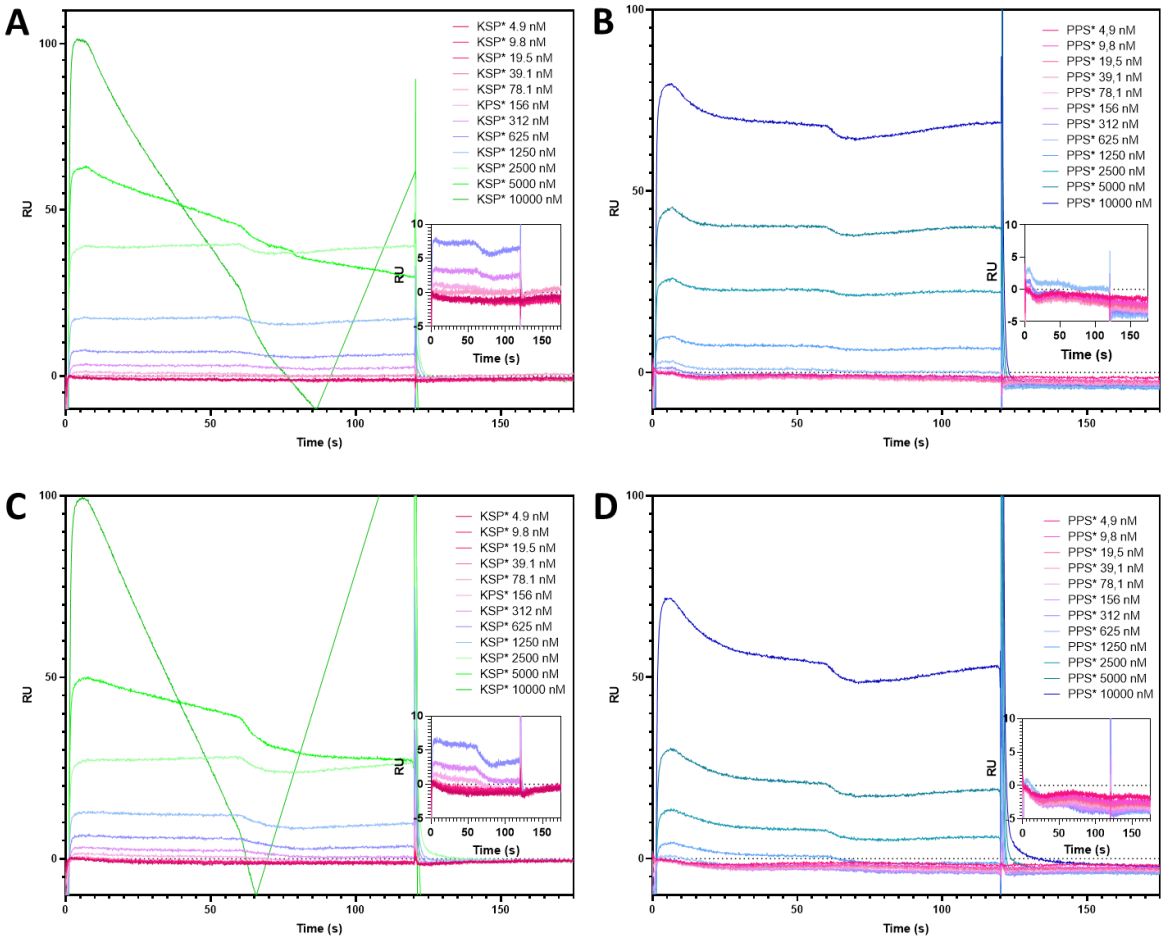

Figure 6. SPR analysis of immobilised HER2 on the Cytiva Sensor Chip SA to serially diluted KSP* and PPS*. Biotinylated HER2 with long spacer on primary amines (**A, B**) or with Avitag on C-terminus (**C,D**) was immobilised on the chip with levels of approximately 2000 and 3000 RU, respectively. The chip surface was regenerated with running buffer (PBS-T) after 120 seconds of association time. The sensorgrams of lower concentrations are magnified in the insets of each graph.

To conclude, these results indicate that KSP* binds to the immobilised HER2 as evidenced by the difference in sensorgrams compared to the scrambled control peptide. However, the obtained binding curves in the current conditions are inadequate for proper determination of the affinity.

DISCUSSION

In this study, we evaluated the binding of ligands to a target protein with two methods: magnetic beads-based fluorescence binding assay and surface plasmon resonance.

Evaluation of binding affinity with magnetic beads-based fluorescence binding assay

In the magnetic beads-based binding assay, we were able to obtain binding curves and consistent affinities for the KSP* and its PEGylated variant, within the same nanomolar ranges as the reported values[19]. We found that none of the six peptides have binding affinities that surpass the reference. On the other hand, the data appears to be rather skewed; with large standard errors and ambiguously fitted curves. To obtain consistent and accurate measurements while ensuring that the ligand-bound beads are washed properly has been rather challenging throughout the assay. It is plausible that this could be the major reason for the large standard deviations between replicate datapoints. Inadequate washing can result in inaccurate measurements, while too many washes come with the increasing risk of various experimental errors such as non-uniform pipetting or accidental aspiration of the beads. Furthermore, as the initial state of equilibrium is disturbed during washing, the longer and more often the beads are washed, the more bound ligands could potentially dissociate. For ligands with strong affinities, such as

the KSP* peptide, this does not pose much of a problem, but it could be detrimental for weaker binders[20,25]. Using higher washing volumes could reduce the amount of handling, however this is limited to the volume of the microplate wells. Alternatively, automated pipetting or an optimised vacuum filtration system, as previously used by Hattori et al., could reduce the washing duration while minimising experimental errors.

It was mentioned that the beads for the non-specific binding control were different from the one used for the total binding. While this technically makes the control unsuitable for baseline subtraction to determine the specific binding, they were made from the same materials and in the same size. Thus, it can provide a close estimation of the non-specific binding. As this was a pre-screen of potential drug candidates *in vitro* and not *in vivo*, the control gave us an idea of the sticky properties (tendency to adhere to any surface) of certain peptides rather than an absolute value of specificity.

With these preliminary results, none of the six promising peptides from the library are good ligands to HER2. We have yet to await the results of the remaining peptides of the library. Further experiments with improved protocols are required to confirm current data and to perform a comparison to other assays, such as fluorescence polarisation assay, cell-based binding assays or SPR.

Evaluation of binding affinity with surface plasmon resonance

As mentioned, SPR is a highly sensitive and accurate method that is able to characterise the interaction of ligands and proteins. The ultrasensitivity also comes with the care and responsibility to use extremely pure samples and reagents. As such, even the slightest change in composition of the running buffer due to different batch sources can cause a noticeable change in signal, especially when the maximum obtainable signal is already low.

Although our initial aim was to gain sufficient SPR signal, sensorgrams with signal as low as 1 RU is theoretically sufficient enough for SPR measurements of small molecules on the Biacore T100[26,27]. However, the accurate determination of K_D at such low signal is obstructed by the relatively high non-specific binding of the compounds to the reference. The main concern therefore should be shifted to reduce non-specific binding. The effect of BSA, Tween-20, DMSO, salt and pH on non-specific binding should be carefully investigated to determine the most optimal running buffer [28]. One could also reduce the stickiness of the peptides by removing the Cy5.5 fluorescent dye, as it is not necessary for measurement of the binding. However, it would make the data less comparable to reported values and data in which labelled versions were used.

While the aforementioned ideas could slightly improve signal quality, it is also likely that the amount of remaining salts left in the purified samples can significantly affect the shape and quality of the sensorgrams. Despite our careful handling of the samples, we suspect that the sheer size difference of peptides compared to the immobilised protein makes it very challenging to conduct binding studies using SPR. One should therefore consider the cost-effectivity of SPR for small-molecule studies.

CONCLUSIONS

We have successfully synthesized a library of promising peptides against HER2. Six members of the library have been evaluated by a magnetic beads-based fluorescence assay and determined affinities ranging from ~40 nM to ~2 μM. Due to reproducibility issues and the ambiguity of the data, the obtained values need to be further ascertained with optimised conditions.

SPR measurements of reference peptide KSP* to immobilised HER2 produced unusual binding sensorgrams. The effects of buffer composition and sample preparation needs to be further investigated in order to obtain more reliable results.

ACKNOWLEDGEMENTS

I would like to thank the RadioPharmaceutical group for allowing me to work on this project and Yann and Priciana for their great guidance and supervision. Also, many thanks to Joyce and Charlie of the Molecular Genetics department for their teaching and feedbacks on the SPR experiments.

REFERENCES

1. Sung, H. *et al.* Global Cancer Statistics 2020: GLOBOCAN Estimates of Incidence and Mortality Worldwide for 36 Cancers in 185 Countries. *CA Cancer J Clin* **71**, 209–249 (2021).
2. Rauser, S. *et al.* Classification of HER2 receptor status in breast cancer tissues by MALDI imaging mass spectrometry. *J Proteome Res* **9**, 1854–1863 (2010).
3. Citri, A. & Yarden, Y. EGF-ERBB signalling: towards the systems level. *Nat Rev Mol Cell Biol* **7**, 505–516 (2006).
4. Yarden, Y. & Sliwkowski, M. X. Untangling the ErbB signalling network. *Nat Rev Mol Cell Biol* **2**, 127–137 (2001).
5. King, C. R., Kraus, M. H. & Aaronson, S. A. Amplification of a novel v-erbB-related gene in a human mammary carcinoma. *Science* **229**, 974–976 (1985).
6. Gutierrez, C. & Schiff, R. HER 2: Biology, Detection, and Clinical Implications. *Arch Pathol Lab Med* **135**, 55 (2011).
7. Yarden, Y. Biology of HER2 and its importance in breast cancer. *Oncology* **61 Suppl 2**, 1–13 (2001).
8. Larsimont, D. *et al.* Comparison of HER-2 status between primary breast cancer and corresponding distant metastatic sites. *Annals of Oncology* **13**, 1036–1043 (2002).
9. Turner, N. H. & di Leo, A. HER2 discordance between primary and metastatic breast cancer: assessing the clinical impact. *Cancer Treat Rev* **39**, 947–957 (2013).
10. L, M. Theranostics: A Unique Concept to Nuclear Medicine. *Archives of Cancer Science and Therapy* **1**, 001–004 (2017).
11. Tamura, K. *et al.* Trastuzumab deruxtecan (DS-8201a) in patients with advanced HER2-positive breast cancer previously treated with trastuzumab emtansine: a dose-expansion, phase 1 study. *Lancet Oncol* **20**, 816–826 (2019).
12. Ulaner, G. A. *et al.* First-in-Human Human Epidermal Growth Factor Receptor 2-Targeted Imaging Using 89 Zr-Pertuzumab PET/CT: Dosimetry and Clinical Application in Patients with Breast Cancer. *J Nucl Med* **59**, 900–906 (2018).
13. Kenny, L. M. *et al.* The HERPET study: Imaging HER2 expression in breast cancer with the novel PET tracer [18F]GE-226, a first-in-patient study. *J Cl Onc* **40**, 3069–3069 (2022).
14. Janeway C. A. Jr, Travers P., Walport M., *et al.* Immunobiology: The Immune System in Health and Disease. 5th edition. - The structure of a typical antibody molecule. *New York: Garland Science* (2001).
15. Shadidi, M. & Sioud, M. Selective targeting of cancer cells using synthetic peptides. *Drug Resistance Updates* **6**, 363–371 (2003).
16. Pilot Imaging Study With 89Zr-Trastuzumab in HER2-positive Metastatic Breast Cancer Patients - Full Text View - ClinicalTrials.gov. https://clinicaltrials.gov/ct2/show/NCT01420146.
17. Sun, X. *et al.* Peptide-based imaging agents for cancer detection. *Adv Drug Deliv Rev* **38** 110–111 (2017).
18. Ducharme, M. & Lapi, S. E. Peptide Based Imaging Agents for HER2 Imaging in Oncology. *Mol Imaging* **19**, 1-10 (2020).
19. Joshi, B. P. *et al.* Design and Synthesis of Near-Infrared Peptide for in Vivo Molecular Imaging of HER2. *Bioconjug Chem* **27**, 481-494 (2016).
20. Jarmoskaite, I., Alsadhan, I., Vaidyanathan, P. P. & Herschlag, D. How to measure and evaluate binding affinities. *Elife* **9**, 1–34 (2020).
21. Stoddart, L. A., White, C. W., Nguyen, K., Hill, S. J. & Pfleger, K. D. G. Fluorescence- and bioluminescence-based approaches to study GPCR ligand binding. *Br J Pharmacol* **173**, 3028-3037 (2016).
22. Motulsky, H. J. & Neubig, R. R. Analyzing Binding Data. *Curr. Protoc. Neurosci.* **52**, 7.5.1-7.5.65 (2010)

23. Markey, F. Principles of Surface Plasmon Resonance. In: Nagata, K., Handa, H. (eds) Real-Time Analysis of Biomolecular Interactions.) Springer, Tokyo. pp. 13-22 (2000)
24. Bakhtiar, R. Surface plasmon resonance spectroscopy: A versatile technique in a biochemist's toolbox. *J Chem Educ* **90**, 203–209 (2013).
25. Pollard, T. D. MBOC technical perspective: A guide to simple and informative binding assays. *Mol Biol Cell* **21**, 4061–4067 (2010).
26. Zhukov, A. *et al.* Biophysical Mapping of the Adenosine A 2A Receptor. *J. Med. Chem* **54**, 4312–4323 (2011).
27. Data file. Biacore ™ T200. Cytiva Life Sciences (2022) https://cdn.cytivalifesciences.com/api/public/content/digi-23615-original
28. Practice Guide. Knowling, S. Best Practice Guide: Minimizing the Effects of Non-specific Binding. Sartorius (2022). https://www.sartorius.com/download/1176984/octet-sf3-avoid-non-specific-binding-best-practice-guide-en-1--data.pdf

SUPPLEMENTARY MATERIALS

		1	2	3	4	5	6	7	8	9	10
1	KSPNPRF*	**-187.545**	-168.579	-163.977	-163.294	-159.228	-157.890	-156.891	-155.355	-154.345	-154.330
3	**3**	YSQPQPQRF*	**-206.548**	-196.529	-196.444	-195.497	-195.207	-192.053	-191.382	-189.845	-189.818
4	**3'**	FRQPQPQSY*	**-215.498**	-197.316	-193.036	-191.398	-191.335	-187.494	-185.428	-184.781	-183.338
7	**6**	*CFSQPQPQRFC	**-221.521**	**-219.097**	**-209.194**	**-203.915**	**-201.793**	**-200.711**	**-192.733**	**-190.577**	**-189.891**
8	**6'**	CFRQPQPQSFC*	-251.513	-239.653	-204.671	-197.346	-196.550	-193.430	-193.399	-189.799	-189.212
9	**6BIS**	FSQPQPQRFC*	**-205.029**	-195.995	-194.055	-193.242	-192.678	-192.434	-191.171	-190.776	-190.761
23	**5**	YQPQPRF*	**-223.543**	**-204.708**	**-195.670**	**-189.712**	**-189.340**	**-187.581**	**-186.305**	**-185.315**	**-184.661**
28	**7**	*YQQPQPQRF	**-224.070**	-192.145	-191.493	-190.156	-188.958	-186.553	-186.066	-183.716	-183.367
44	**9**	*FRQPQPRF	**-207.700**	**-204.436**	**-193.335**	**-191.753**	**-190.351**	**-186.542**	**-185.337**	**-183.440**	**-182.540**
46	**10**	*FRQPQPQRF	**-207.680**	**-205.358**	**-199.330**	**-199.210**	**-198.191**	**-193.672**	**-193.618**	**-191.588**	**-190.763**

Table S1. Anti-HER2 peptide library. Top 10 conformations of each peptide and its docking scores versus HER2 performed in HPEP dock. The one at the top is the reference KSP* peptide, and below is a selection of 9 PQP peptides. The star (*) denotes labelling position at the C- or N terminal site.

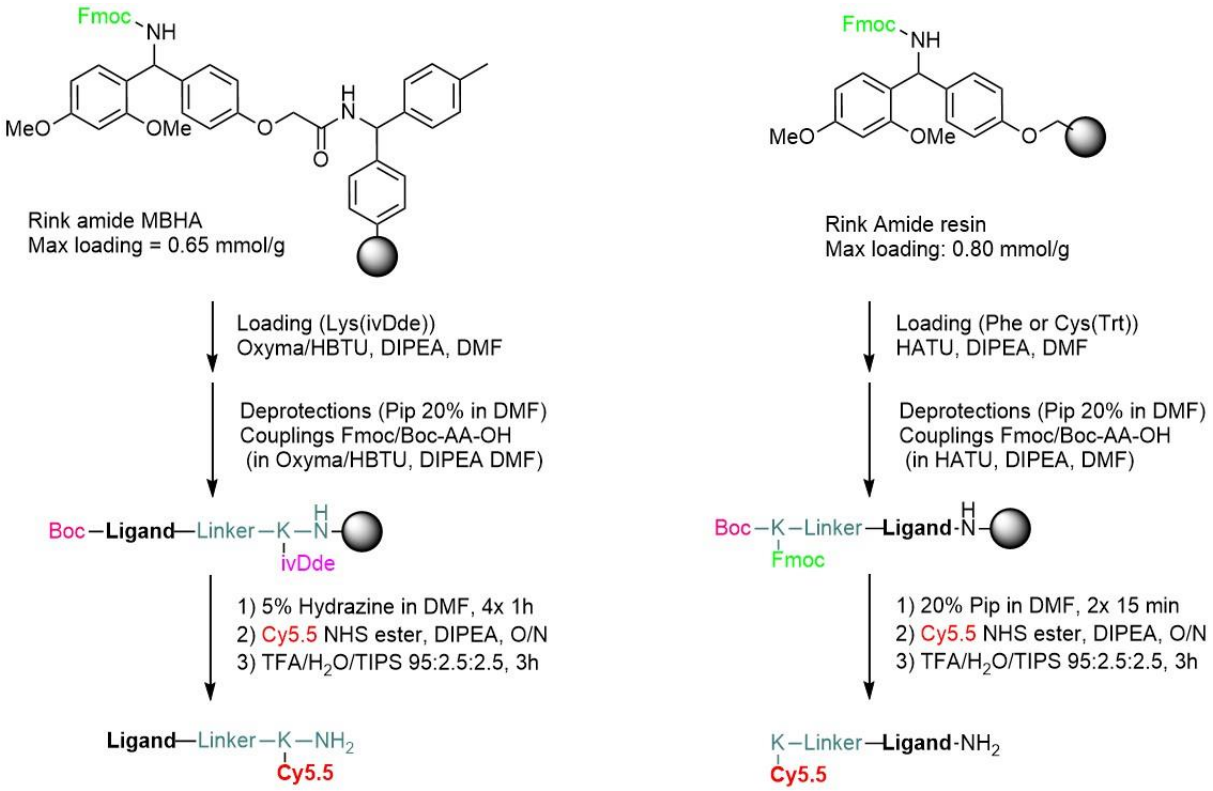

Figure S1. General synthesis scheme of Cy5.5 conjugated peptides. Cy5.5 is linked to the ligand (peptide sequence) on either the N-terminus or C-terminus and synthesized according to the strategies on the left and right, respectively.

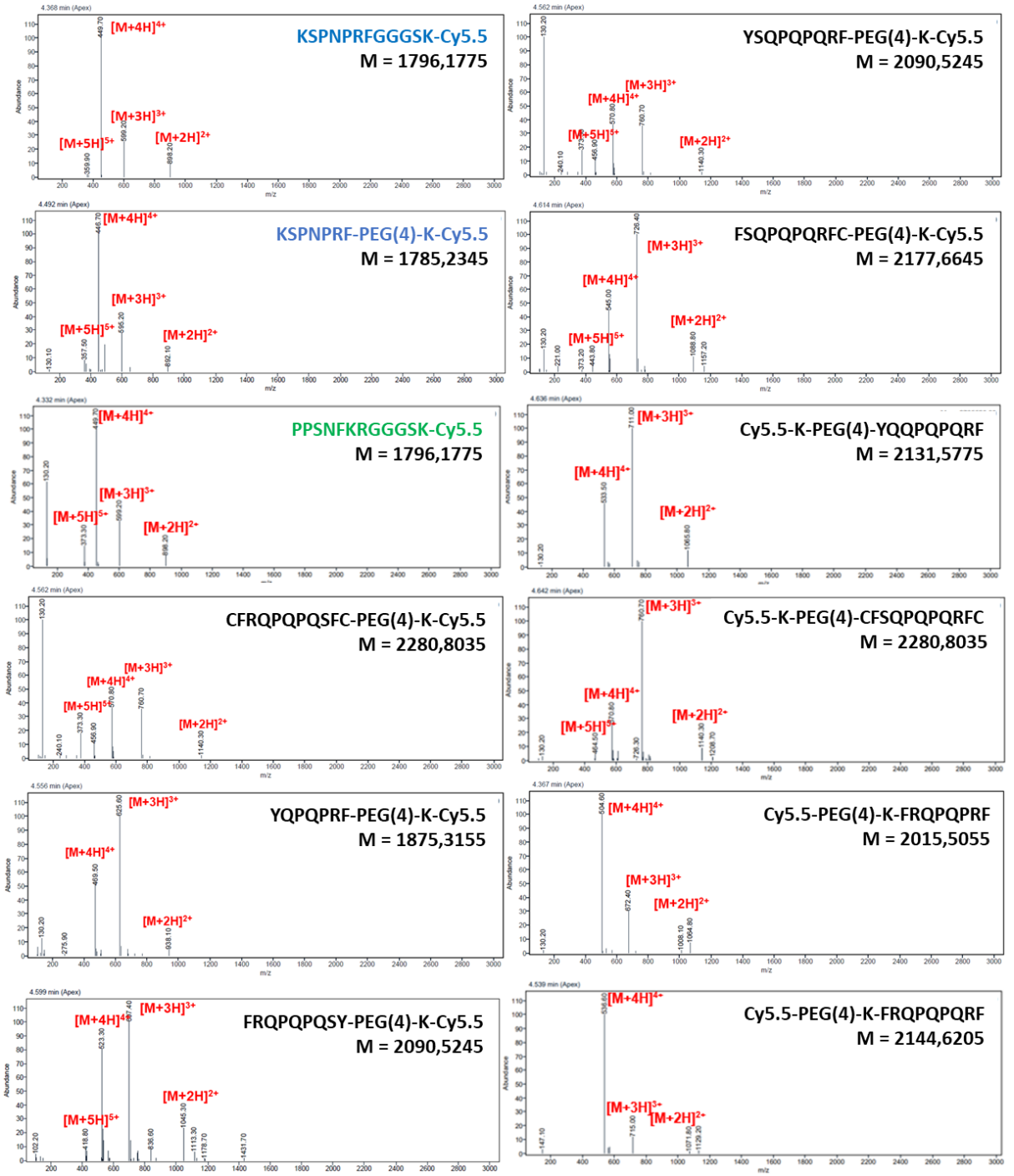

Figure S2. Mass spectrometry analysis of Cy5.5 labelled peptides. Purified reference peptides (blue), scrambled control peptide (green) and the library of promising peptides (black) were characterised by ESI-MS in positive ion mode. The experimental mass-to-charge (m/z) ratios correspond to the expected values.

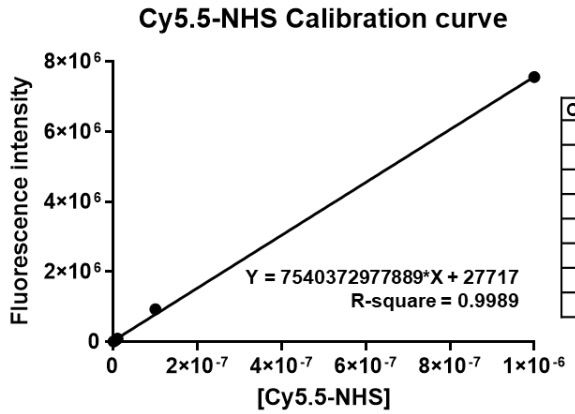

Concentration (M)	Fluorescence (AU)		
0,000001	7346166	7756724	7558323
1e-007	857320	968993	957555
1e-008	89073	92789	94534
5e-009	40211	44303	40918
1e-009	11366	11411	11181
5e-010	6776	7663	6687
1e-010	4162	4887	3863
5e-011	3243	3582	3353

Figure S3. Standard calibration line of Cy5.5 NHS ester. Fluorescence data show triplicate measurements of three independent dilutions of the dye in PBS + 0.05% Tween-20.

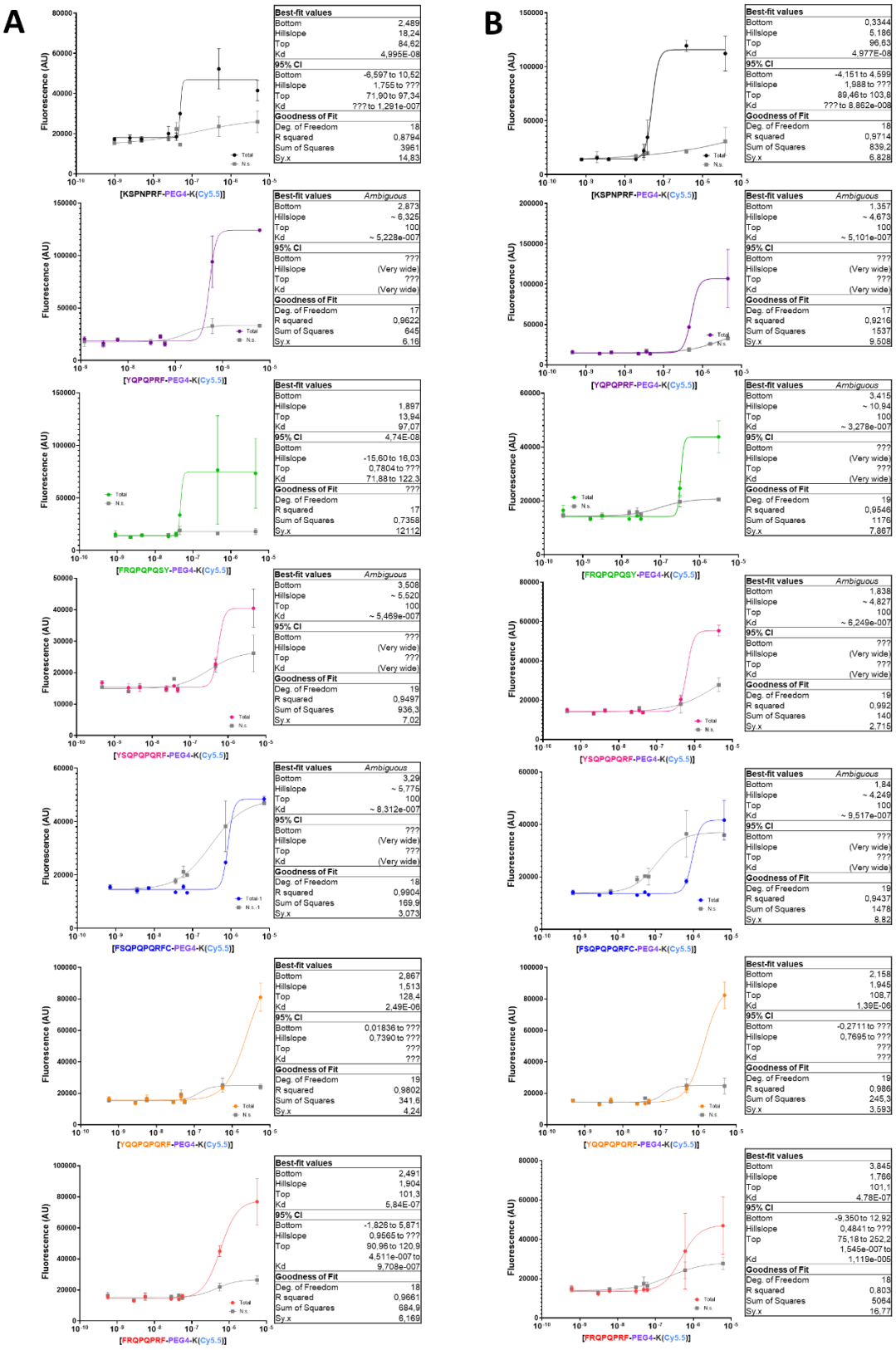

Figure S4. Binding of reference and peptide library to HER2. Expanding on Figure 3, total and non-specific binding of the reference and peptide library to HER2 was detected via fluorescence and measured in triplicate on two independent days, each shown separately in (**A**) and (**B**). Curves were fitted via a linear regression of a 1:1 binding model with the errors showing s.d. The calculated parameters and statistics of the total binding curves are summarised in corresponding tables.

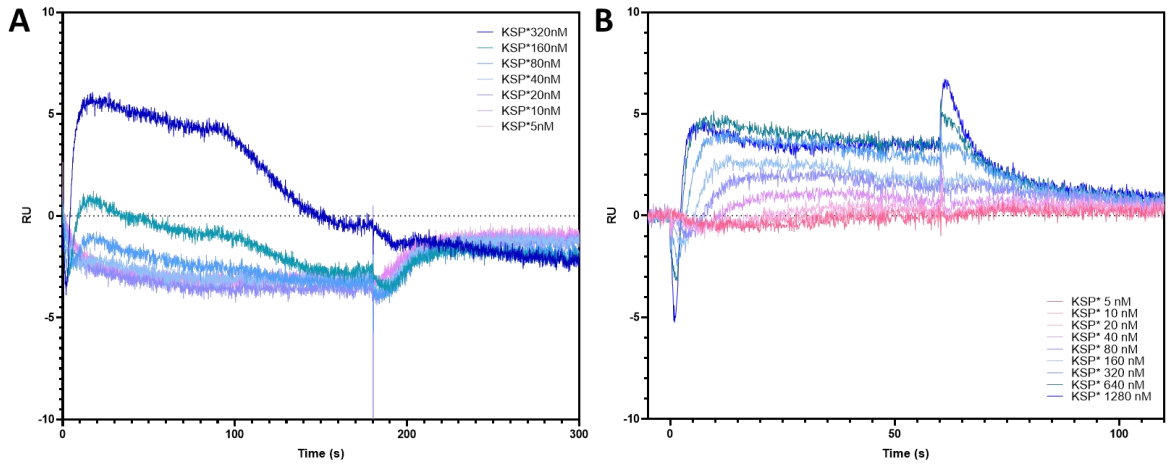

Figure S5. SPR analysis of KSP* to immobilised HER2. PBS-T was used as running buffer to measure the binding of KSP* to HER2. After each association phase, the chip surface was regenerated with (**A**) 10 mM glycine.HCl (pH 1.5) after contact time of 180 seconds, or (**B**) running buffer, after 60 seconds.

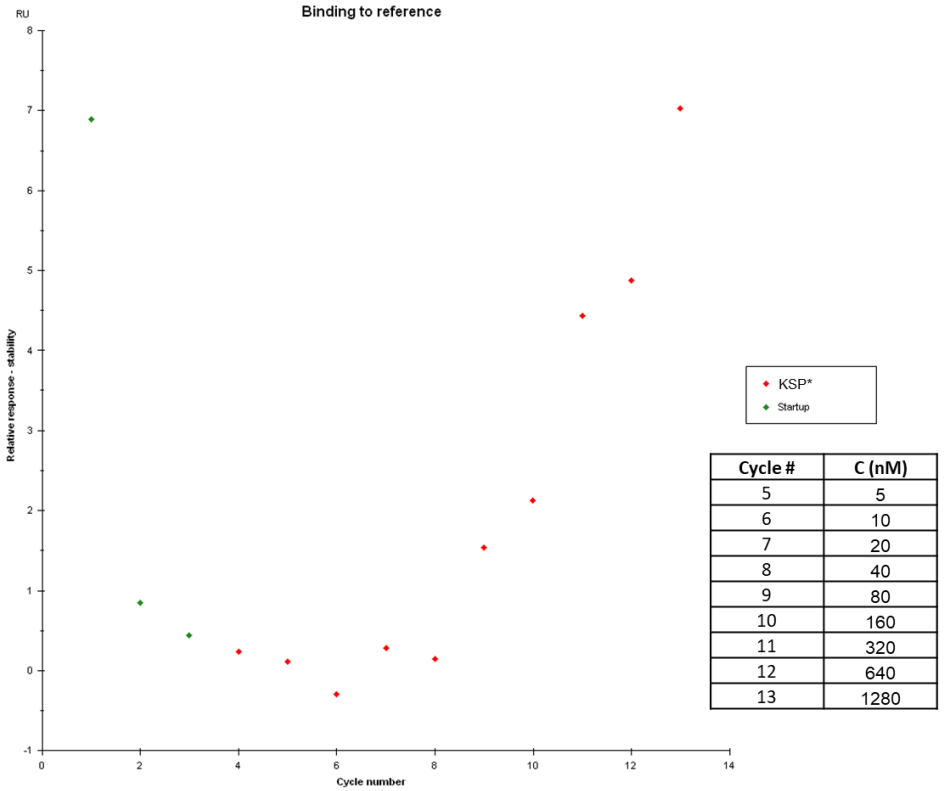

Cycle #	C (nM)
5	5
6	10
7	20
8	40
9	80
10	160
11	320
12	640
13	1280

Figure S6. Binding of KSP* to the SPR reference flow cell. Each datapoint refers to the binding signal increase relative to initial baseline of the reference flow cell after each measurement cycle. Analysis generated in the Biacore T100 software.